

Prenatal androgen treatment does not alter the firing activity of hypothalamic arcuate kisspeptin neurons in female mice

Amanda G. Gibson², Jennifer Jaime², Laura L. Burger¹, Suzanne M. Moenter^{1,3,4,5}

Departments of Molecular & Integrative Physiology¹, Neuroscience Graduate Program², Internal Medicine³, Obstetrics & Gynecology⁴, and the Reproductive Sciences Program⁵, University of Michigan, Ann Arbor, MI, 48109, USA

Short title: Arcuate kisspeptin neuron activity in female mice

Corresponding author, Suzanne M Moenter, Ph.D., Department of Molecular and Integrative Physiology, University of Michigan, 7725 Med Sci II, 1137 E. Catherine St, Ann Arbor, MI 48109-5622

734-647-1755 (voice), 734-936-8813 (fax) smoenter@umich.edu

Number of figures: 5

Number of tables: 6

Number of extended data: 1

Number of words: abstract 249, introduction 588, discussion 1655.

Acknowledgements: Supported by National Institute of Health/Eunice Kennedy Shriver National Institute of Child Health and Human Development P50HD028934 and R01HD104345. AGG was supported by the National Defense Science and Engineering Graduate Fellowship Program. We thank Elizabeth Wagenmaker for expert technical assistance and Joshua Gibson for computational guidance.

Conflict of interest: The authors declare no competing financial interests.

Abbreviations: ACSF, artificial cerebral spinal fluid; ANOVA, analysis of variance; ARC, hypothalamic arcuate nucleus; DHT, dihydrotestosterone; FSH, follicle-stimulating hormone; GABA, gamma-aminobutyric acid; GFP, green fluorescent protein; GnRH, gonadotropin-releasing hormone; KNDy, neurons co-expressing kisspeptin, neurokinin B and dynorphin; LH, luteinizing hormone; PCOS, polycystic ovary syndrome; PNA, prenatally androgenized; PND, postnatal day; SK, senktide; Std resid, standardized residual

1 **Abstract**

2 Neuroendocrine control of reproduction is disrupted in many individuals with polycystic ovary
3 syndrome, who present with increased luteinizing hormone (LH), and presumably gonadotropin-
4 releasing hormone (GnRH), release frequency, and high androgen levels. Prenatal
5 androgenization (PNA) recapitulates these phenotypes in primates and rodents. Female
6 offspring of mice injected with dihydrotestosterone (DHT) on gestational D16-18 exhibit
7 disrupted estrous cyclicity, increased LH and testosterone, and increased GnRH neuron firing
8 rate as adults. PNA also alters the developmental trajectory of GnRH neuron firing rates,
9 markedly blunting the prepubertal peak in firing that occurs in 3wk-old controls. GnRH neurons
10 do not express detectable androgen receptors and are thus probably not the direct target of
11 DHT. Rather, PNA likely alters GnRH neuronal activity by modulating upstream neurons, such
12 as hypothalamic arcuate neurons co-expressing kisspeptin, neurokinin B (gene *Tac2*), and
13 dynorphin, aka KNDy neurons. We hypothesized PNA treatment changes firing rates of KNDy
14 neurons in a similar age-dependent manner as GnRH neurons. We conducted targeted
15 extracellular recordings (0.5-2h) of *Tac2*-identified KNDy neurons from control and PNA mice at
16 3wks of age and in adulthood. About half of neurons were quiescent ($<0.005\text{Hz}$). Long-term
17 firing rates of active cells varied, suggestive of episodic activity, but were not different among
18 groups. Short-term burst firing was also similar. We thus reject the hypothesis that PNA alters
19 the firing rate of KNDy neurons. This does not preclude altered neurosecretory output of KNDy
20 neurons, involvement of other neuronal populations, or *in-vivo* networks as critical drivers of
21 altered GnRH firing rates in PNA mice.

22 **Significance statement**

23 Prenatal androgenization (PNA) recapitulates key aspects of the common reproductive disorder
24 polycystic ovary syndrome. It is postulated that disruptions in the episodic pattern of
25 gonadotropin-releasing hormone (GnRH) secretion in part underly this disorder, yet GnRH
26 neurons do not express androgen receptor to respond directly to elevated androgens. A
27 population of kisspeptin, neurokinin B, and dynorphin-expressing (KNDy) neurons in the
28 hypothalamic arcuate nucleus are thought to regulate pulsatile GnRH release and some
29 express androgen receptor. We did not find evidence, however, that PNA altered spontaneous
30 activity of KNDy neurons before puberty at 3wks of age or in adulthood. This suggests that PNA
31 likely acts through other components of the broader hypothalamic network to change the
32 patterns of GnRH release.

33 **Introduction**

34 Gonadotropin-releasing hormone (GnRH) regulates the secretion of the gonadotropins
35 luteinizing hormone (LH) and follicle-stimulating hormone (FSH) from the anterior pituitary.
36 GnRH is released in an episodic manner that varies in frequency through the female
37 reproductive cycle (Levine and Ramirez, 1982; Moenter et al., 1991). Lower frequency favors
38 synthesis and release of FSH over LH and is important for recruiting ovarian follicles and their
39 subsequent maturation, whereas higher pulse frequency in the mid-late follicular phase favors
40 LH, which drives androgen synthesis (Haisenleder et al., 1991; Wildt et al., 1981). Failure to
41 vary the frequency of GnRH release is thought to be a key neuroendocrine phenotype of the
42 reproductive disorder polycystic ovary syndrome (PCOS).

43 PCOS is a complex spectrum of reproductive and metabolic phenotypes with postulated genetic
44 and environmental causes. Patients with PCOS often exhibit a persistently high LH (and
45 presumably GnRH) pulse frequency, leading to disrupted follicle maturation and ovulation.
46 Increased LH stimulation also drives hyperandrogenism (Dumesic et al., 2015; McCartney et al.,
47 2002). To investigate the etiology of the disorder, animal models are needed for experimental
48 manipulations and measurements that cannot be conducted in humans. Elevated prenatal
49 androgen exposure (PNA) recapitulates PCOS-like reproductive phenotypes in many species
50 including non-human primates (Abbott et al., 2008, 2017, 2019; Dumesic et al., 1997), sheep
51 (Birch et al., 2003; Veiga-Lopez et al., 2008), and rodents (Foecking et al., 2005; Sullivan and
52 Moenter, 2004). In adult PNA mice, LH pulse frequency (Moore et al., 2015) and GnRH-neuron
53 action potential firing frequency (Roland and Moenter, 2011) are both increased. PNA in mice
54 also alters the developmental trajectory of GnRH-neuron firing frequency, which is interesting as
55 aspects of PCOS may emerge around the pubertal transition (McCartney et al., 2002;
56 Rosenfield, 2007). Specifically, in control mice, the firing frequency peaks at 3wks of age before
57 decreasing to adult levels (Dulka and Moenter, 2017). In contrast, the firing frequency in PNA
58 female mice did not vary with age, and it was lower than control mice at 3wks, distinct from the
59 increase observed in PNA adults (Dulka and Moenter, 2017; Sullivan and Moenter, 2004)

60 The mechanisms by which PNA alters the activity of GnRH neurons are not completely
61 understood. These neurons do not express detectable levels of androgen receptor (Herbison et
62 al., 1996), thus it is likely that upstream neuronal populations are involved in regulating their
63 firing patterns. One such population is in the hypothalamic arcuate nucleus, specifically neurons
64 that co-express kisspeptin, neurokinin B, and dynorphin (KNDy neurons). KNDy neurons are

65 posited to be involved in the control of pulsatile GnRH, and subsequent LH, secretion (Clarkson
66 et al., 2017; S. Y. Han et al., 2015; McQuillan et al., 2019). KNDy neurons express receptors for
67 gonadal steroids, including androgen receptor (Smith et al., 2005), and could serve as the site
68 of steroidal feedback that alters GnRH neuron activity and/or a site of action for PNA exposure
69 (Caldwell et al., 2017; Oakley et al., 2009; Vanacker et al., 2017; Walters et al., 2018).

70 We hypothesized that PNA treatment would alter the firing frequency of KNDy neurons in an
71 age-dependent manner similar to that of GnRH neurons. We tested this by assessing the effect
72 of PNA on the spontaneous firing frequency of KNDy neurons in prepubertal 3wk-old and adult
73 female mice through long-term extracellular recordings. Specifically, we postulated that PNA
74 treatment would increase KNDy-neuron activity relative to controls in adults but reduce activity
75 relative to controls in 3-wk old mice. We also predicted that 3wk-old control mice would exhibit
76 increased KNDy-neuron firing frequency relative to control adults and 3wk-old PNA mice.

77 **Materials and Methods**

78 *Animals* Mice expressing enhanced green fluorescent protein (GFP) under the control of Tac2
79 promoter (Tac2-GFP, BAC transgenic mice (015495-UCD/STOCK Tg [Tac2-EGFP]381Gsat,
80 Mouse Mutant Regional Resource Center (<http://www.mmrrc.org/>) were used to identify KNDy
81 neurons for recording. In mice, *Tac2* encodes neurokinin B, which is co-expressed with
82 kisspeptin and dynorphin in KNDy neurons. Tac2-GFP-identified cells in brain slices used for
83 recording also express kisspeptin and/or dynorphin at high percentages, supporting their identity
84 as KNDy neurons (Ruka et al., 2013). Mice were maintained in a 14h:10h dark photoperiod
85 (lights on at 0300 Eastern Standard Time) and had *ad libitum* access to water and either Harlan
86 2919 chow during pregnancy/lactation or 2916 chow for maintenance. All animal procedures
87 were performed in accordance with the University of Michigan Institutional Animal Care and Use
88 Committee's regulations.

89 To generate experimental mice, a Tac2-GFP female and CD1 female mice were bred with a
90 C57B/6 male and monitored daily for a copulatory plug (day 1 of pregnancy). The CD1 dam
91 assists in providing maternal care and nutrition. On days 16-18 of pregnancy, dams were
92 injected subcutaneously with 225 μ g/day of dihydrotestosterone (DHT) or sesame oil as vehicle.
93 Control offspring from dams for whom timing of pregnancy could not be clearly established were
94 also included in studies without injections; firing rate from these mice did not differ from vehicle-
95 treated mice (treatment: $F_{(1, 22)} = 2.114$, $p = 0.160$; interaction of age and treatment: $F_{(1, 22)} =$
96 0.237 , $p = 0.631$). Experiments were conducted on female offspring prior to weaning at 3 weeks

97 of age (PND 18-21) or in adulthood (PND 66-152; median 133). PNA status was confirmed by
98 anogenital distance and estrous cyclicity in adults. Anogenital distance was measured with
99 digital calipers on 2-3 successive days and averaged for each mouse. Estrous cyclicity was
100 assessed via vaginal cytology and studies on adult females were done on diestrus. Cycle stage
101 was confirmed with uterine mass; one DHT-treated mouse was excluded due to a uterine mass
102 of 136.2mg, suggestive of incorrect cycle identification based on vaginal cytology.

103 *Brain Slice Preparation* All solutions were bubbled with 95% O₂/5% CO₂ for at least 15min prior
104 to tissue exposure and throughout the procedures. The brain was rapidly removed and cooled
105 for 60s in ice-cold sucrose saline solution containing (in mM): 250 sucrose, 3.5 KCL, 26
106 NaHCO₃, 10 D-glucose, 1.25 Na₂HPO₄, 1.2 MgSO₄, and 3.8 MgCl₂. Coronal slices (300 μm)
107 through the hypothalamic region, including the ARC, were cut with a Leica VT1200S (Leica
108 Biosystems, Buffalo Grove, IL). Slices were incubated for 30min at room temperature in 50%
109 sucrose saline and 50% artificial cerebral spinal fluid (ACSF) containing (in mM): 135 NaCl, 3.5
110 KCl, 26 NaHCO₃, 10 D-glucose, 1.25 Na₂HPO₄, 1.2 MgSO₄, and 2.5 CaCl₂ (pH 7.4). The slices
111 were then held in 100% ACSF at room temperature for between 0.5 to 5.5h before recording.
112 No differences in results were attributable to duration post brain slice preparation.

113 *Electrophysiological recording* To evaluate the long-term firing patterns of KNDy neurons with
114 minimal disruption of the cell's intrinsic properties, targeted single-unit extracellular recordings
115 were conducted (Alcami et al., 2012; Nunemaker et al., 2003). Individual slices were transferred
116 to a recording chamber mounted on the stage of an Olympus BX51WI upright fluorescent
117 microscope. A constant perfusion of ACSF at a rate of 3mL/min was established with a
118 MINIPULS 3 peristaltic pump (Gilson, Middleton, WI). The chamber was maintained at a
119 temperature of 29-32°C with an inline heating system (Warner Instrument Corporation, Hamden,
120 CT). ACSF was replaced every hour.

121 Recording electrodes (resistance 2-4MΩ) were pulled from borosilicate glass (Schott no. 8250;
122 World Precision Instruments, Sarasota, FL) using a Sutter P-97 puller (Sutter Instrument,
123 Novato, CA). The pipettes were filled with a HEPES-buffered pipette solution containing (in
124 mM): 150 NaCl, 10 HEPES, 10 D-glucose, 2.5 CaCl₂, 1.3 MgCl₂, and 3.5 KCl, pH7.4. At the
125 surface of the brain slice, a small amount of negative pressure was applied to bring the pipette
126 in contact with tissue, facilitating the later formation of a low-resistance seal (<100MΩ) between
127 the pipette and neuron (Alcami et al., 2012). Recordings were made with one channel of an
128 EPC10 dual patch-clamp amplifier using PatchMaster software (HEKA Elektronik, Lambrecht,

129 Germany). Cells were held in voltage-clamp with a 0mV pipette holding potential. Seal
130 resistance was checked every 10-15min by measuring response to a 5mV hyperpolarizing step
131 between series. Data were acquired at 10kHz and filtered at 5kHz.

132 Recording duration ranged from 0.5 to 2.6h (mean \pm SEM 71.7 \pm 2.9min; median 60min). If a cell
133 was not firing at the conclusion of a recording session, either high-potassium ACSF (20 mM K⁺)
134 or the neurokinin 3 receptor agonist senktide (100nM; Phoenix Pharmaceuticals, Burlingame,
135 CA) was bath-applied. If a cell failed to respond to these stimuli with increased firing, recording
136 integrity could not be verified and data analysis was truncated to the last action current.
137 Response to senktide was quantified by comparing the spontaneous firing frequency for the
138 5min prior to addition of senktide to the ACSF to the firing frequency for 5min, beginning 2min
139 after senktide reached the bath to allow time for the drug to equilibrate in the chamber and
140 penetrate the slice. This 2min delay was chosen based on the onset of and peak senktide
141 response across cells.

142 *Analysis* Event detection was completed using IgorPro8 (WaveMetrics, Inc., Lake Oswego, OR)
143 utilizing custom routines, and all events were manually confirmed. The average spontaneous
144 firing rate was calculated for each cell as total events/recording duration. The short-term
145 patterns of neuronal activity were also assessed with custom IgorPro8 routines. Repetitive,
146 grouped firing events are referred to as “bursts” for analysis. To be considered part of a burst, a
147 firing event must occur within a defined “burst window” after the previous event. The burst
148 window for analysis of these KNDy neurons was identified by varying the burst window from
149 0.01s to 1s in 10ms intervals and selecting the burst window that captures the maximal burst
150 frequency for the control cells; this was 230ms as in prior reports (Vanacker et al., 2017). At the
151 selected burst window, the software characterizes each event as belonging to a burst or as a
152 single spike, then calculates the following parameters: burst frequency, burst duration, intraburst
153 interval, spikes per burst, single spike frequency, and interevent interval. Burst duration and
154 spikes per burst are the averages for all bursts from a given cell. Intraburst interval is the
155 average of intervals between spikes in a burst, whereas interevent interval is the average of
156 intervals greater than the burst window and can occur between bursts, between single spikes or
157 between single spikes and bursts. Short breaks in the recording (typically <2s) occur at 10-15
158 min intervals to monitor the seal resistance. Intervals that crossed these gaps were not included
159 when calculating cells’ averages. Spikes that occurred within 230ms (i.e., the burst window) of
160 these gaps, or the start or end of the recording, were characterized according to the available

161 information; this could lead to an underestimate of the burst frequency, burst duration, and/or
162 spikes per burst.

163 *PCR to assess arcuate gene expression* Hypothalamic tissue punches were collected to assess
164 the effect of PNA on gene expression. Separate cohorts of mice from those used for recordings
165 were utilized to collect tissue micro-punches from the ARC. A coronal slice was obtained with an
166 adult mouse brain matrix (1mm, Zivic Instruments, Pittsburgh, PA); an initial cut was made just
167 caudal to the optic chiasm, followed by a cut just rostral to the brain stem (2-3 mm thick) for the
168 ARC. Tissue punches were made with a 1.2mm Palkovits punch. Tissue was immediately
169 homogenized in RLT buffer (Qiagen, Valencia, California) containing 2-mercaptoethanol (1%v/v,
170 Sigma), snap frozen, and stored at -80°C. RNA from was extracted with the RNeasy Micro Kit
171 with on column DNasing (Qiagen). 240ng RNA per sample was reverse transcribed with
172 Superscript IV VILO Master Mix (Fisher/Invitrogen). A standard curve of hypothalamic RNA
173 (600, 120, 24, 4.8 and 0ng/20µl) was also reverse transcribed (Ruka et al., 2013). The
174 transcripts for: *Kiss1*, *Kiss1r*, *Pdyn*, *Oprk1*, *Tac2*, *Tacr3*, *Ar*, *Esr1* and *Pgr* were assayed via
175 Taqman quantitative PCR in duplicate with 10ng cDNA. Data were analyzed by the $\Delta\Delta CT$
176 method (Bustin, 2002), normalized to *Actb* and *Syn1* and reported relative to 3wk-CON. Primers
177 and Taqman probes were purchased from Integrated DNA Technologies (Coralville, IA) and are
178 reported in Table 1.

179 *Statistics* Data visualization and analyses were conducted with R (R Core Team, 2019) and
180 RStudio (RStudio Team, 2019) using a combination of open-sourced packages (Chang, 2014;
181 Chang et al., 2020; Fox and Weisberg, 2019; Gohel, 2020b, 2020a; Henry and Wickham,
182 2020b, 2020a; Kassambara, 2020, 2021; Schauburger and Walker, 2020; Schloerke et al.,
183 2020; Wickham et al., 2019, 2020; Wickham and Hester, 2020; Wickham and Seidel, 2020;
184 Wilke, 2020; Xie, 2014, 2015, 2020; Xie et al., 2021; Zhu, 2020) and custom procedures.
185 Additional statistical analyses were conducted with Prism 9 (GraphPad, La Jolla, CA). Data are
186 reported as mean \pm SEM, with median illustrated where indicated. For recordings, n is number of
187 cells; for PNA phenotype confirmation and mRNA quantification, n is number of mice. Normality
188 of the data distribution was evaluated with Shapiro-Wilk. Two-way ANOVA (Type III) was
189 conducted to evaluate the main effects and interactions of age and prenatal treatment.
190 Bonferroni correction for multiple comparisons was used as test is sufficiently robust for non-
191 normally distributed data (Underwood, 1997). The level accepted as significant was set to
192 $p < 0.05$. Statistical tables for two-way ANOVAs report the differences in means and associated

193 95% CI defined for age (adult – 3wk), treatment (PNA – control), and interaction ([adult PNA –
194 adult control] – [3wk PNA – 3wk control]).

195 *Software accessibility* The event detection and burst analysis code described in the paper is
196 freely available online at <https://gitlab.com/um-mip/coding-project>. The R analysis code is freely
197 available online at https://github.com/gibson-amandag/PNA_KNDy. The code is available as
198 Extended Data 1. Analyses were conducted on a MacBook Pro, Early 2015 version, running
199 macOS Catalina 10.15.7 and on a Mac Mini, 2018 version, running macOS Mojave 10.14.6

200 **Results**

201 *PNA characterization* To verify the effects of PNA, anogenital distance, body mass, and estrous
202 cycles were recorded from adult mice and the surviving female littermates of 3wk-old mice
203 where possible. Adult PNA mice had a longer anogenital distance (Figure 1A, statistical
204 parameters in Table 2, control n=17 mice from 10 litters, PNA 23 mice from 11 litters, $p<0.0001$)
205 and larger body mass (Figure 1B, $p=0.026$) than control mice. PNA treatment also altered the
206 distribution of days spent in each estrous cycle stage (Figure 1C, D, $p<0.0001$). PNA mice spent
207 more days in diestrus than expected (standardized residual=7.08) and fewer days in proestrus
208 than expected (standardized residual=-10.11). These results indicate that the PNA treatment
209 was successful.

210 *Spontaneous firing rate* To determine how age and PNA treatment alter the firing activity of
211 KNDy neurons, we conducted targeted, long-term extracellular recordings of Tac2-GFP-
212 identified neurons in the arcuate nucleus of the hypothalamus. These neurons exhibited firing
213 patterns consistent with episodic activity (representative traces in Figure 2A and 2B). About half
214 of recorded Tac2-GFP neurons were quiescent (defined as $<0.005\text{Hz}$). The proportion of
215 quiescent neurons did not vary with age or treatment (Figure 2C; statistical parameters reported
216 in Table 3; 3wk-CON n=11 cells from 7 mice in 5 litters, 3wk-PNA n=22 cells from 12 mice in 6
217 litters, adult-CON n= 15 cells from 10 mice in 6 litters, adult-PNA n=22 cells from 13 mice in 8
218 litters). Neither age nor PNA treatment affected the mean firing frequency of Tac2-GFP neurons
219 over the recording period (Figure 2D).

220 *Response to Senktide* To verify viability of quiescent cells, the neurokinin B receptor agonist
221 senktide was added at the conclusion of a subset of spontaneous recordings (3wk-CON n=8
222 cells from 6 mice in 5 litters, 3wk-PNA n=12 cells from 8 mice in 4 litters, adult-CON n=8 cells
223 from 6 mice in 3 litters, adult-PNA n=14 cells from 10 mice in 6 litters). While performed as a

224 quality check, this test is also biologically relevant as senktide activates firing activity of Tac2-
225 GFP neurons (Ruka et al., 2013), and it is possible that age and treatment alter this. Tac2-GFP
226 neurons responded to senktide with an increase in firing frequency (Figure 3; statistical
227 parameters in Table 4, main effect of time, $p < 0.0001$). This increase was evident in adult-CON
228 ($p = 0.007$), adult-PNA ($p = 0.001$), and 3wk-CON ($p = 0.003$), yet there was not a significant
229 increase for the 3wk-PNA ($p = 0.415$). This suggests that PNA treatment may alter the
230 development of the response to senktide in KNDy neurons.

231 *Short-term firing pattern* Examining the average firing frequency over the duration of the
232 recording could obscure changes in the short-term organization of action potentials that may be
233 more relevant for neurosecretion (Cazalis et al., 1985; Dutton and Dyball, 1979). We thus
234 investigated the effect of age and PNA treatment on short-term firing patterns called bursts.
235 (Figure 4; statistical parameters in Table 5). Because not all cells exhibit burst firing, the n for
236 cells changes for parts B, C and D, and for part F as detailed in the legend. There were no
237 differences due to age or treatment on any parameter other than burst duration. Burst duration
238 was greater in cells from adults than those from 3wk-old mice (Figure 4B; $p = 0.031$). An increase
239 in burst duration could occur as a result of more spikes per burst, and/or a longer intraburst
240 interval. Though it did not reach the level set for statistical significance, the increase in burst
241 duration in adults appears to be driven primarily by increased spikes per burst (Figure 4C;
242 $p = 0.096$) rather than a change in the intraburst interval (Figure 4D; $p = 0.911$).

243 *Development but not PNA affects expression of key transcripts* To examine the effects of age
244 and PNA on steroid receptors and KNDy neuron peptides and receptors in the arcuate nucleus,
245 we quantified mRNA expression of androgen (*Ar*), estrogen (*Esr1*), and progesterone (*Pgr*)
246 receptors and of kisspeptin (*Kiss1*), neurokinin B (*Tac2*), and dynorphin (*Pdyn*), and their
247 corresponding receptors (*Kiss1r*, *Tacr3*, and *Oprk1*, respectively). *Tac2* ($p = 0.0001$) and *Tacr3*
248 ($p < 0.0001$) expression were both increased in adults compared to 3wk-old mice (Figure 5,
249 statistical parameters in Table 6, 3wk-CON n=9 mice, 3wk-PNA n=8 mice, adult-CON n=8 mice,
250 adult-PNA n=7 mice). Similarly, *Ar* ($p < 0.0001$) and *Pgr* ($p < 0.0001$) were increased in the adult
251 arcuate nucleus (Figure 5). PNA treatment did not alter expression of any transcripts, though
252 there were weak trends for PNA to increase expression of *Kiss1r* ($p = 0.091$) and *Pdyn* ($p = 0.071$,
253 Figure 5).

254 **Discussion**

255 Changes in the frequency of GnRH release throughout female reproductive cycles are important
256 for fertility. Patients with PCOS often fail to exhibit these changes, instead displaying a
257 persistently elevated LH, and presumably GnRH, pulse frequency. Here, we tested the
258 hypothesis that prenatal exposure to elevated androgens, a model that recapitulates aspects of
259 PCOS, disrupts the hypothalamo-pituitary-gonadal axis in part by changing the firing activity of
260 KNDy neurons in the arcuate nucleus. Contrary to our hypothesis, neither overall spontaneous
261 activity of KNDy neurons nor most burst characteristics were altered by PNA treatment either
262 before puberty or in adulthood. Expression of *Tac2*, *Tacr3*, *Ar*, and *Pgr* mRNA was greater in
263 the arcuate of adult mice as compared to 3wk mice, but this expression was not impacted by
264 PNA treatment. These findings suggest that changes in KNDy neuron activity alone are not
265 responsible for the altered LH pulse frequency observed with PNA treatment.

266 KNDy neurons have been postulated to be the pulse generator for GnRH release (Clarkson et
267 al., 2017; McQuillan et al., 2019). Kisspeptin increases GnRH release (Glanowska et al., 2014;
268 Messenger et al., 2005) *in vivo* and in brain slices, and increases GnRH neuron activity (S.-K.
269 Han et al., 2005; Pielecka-Fortuna et al., 2008) in brain slices. As the putative pulse generator,
270 KNDy neuron activity would be expected to change in manners that reflect the output of GnRH
271 neurons and LH release. GnRH neuron firing rate changes with development and PNA
272 treatment alters the typical developmental trajectory. Specifically, in GnRH neurons from adults,
273 firing rate is elevated in PNA mice (Roland and Moenter, 2011), whereas firing frequency in
274 cells from PNA mice before puberty at 3wks of age is reduced, because PNA treatment blunts
275 the typical peak in firing that occurs near this age in control mice (Dulka and Moenter, 2017).
276 We expected similar effects in KNDy neurons. Consistent with prior studies in adults, many of
277 the KNDy cells that we recorded were quiescent (de Croft et al., 2012; Frazao et al., 2013; Ruka
278 et al., 2013). Surprisingly, neither age nor PNA treatment altered the mean firing frequency of
279 KNDy neurons. Similarly, effects on short-term burst firing were minimal. These observations
280 suggest that both development and prenatal exposure to androgens alter GnRH neuron activity
281 and release via mechanisms other than changing the activity of KNDy neurons.

282 The elevated LH pulse frequency in patients with PCOS is attributable at least in part to reduced
283 negative feedback actions of progesterone (Pastor et al., 1998). When patients are treated with
284 the anti-androgen flutamide, the suppressive effects of progesterone on LH release are partially
285 restored (Eagleson et al., 2000), suggesting that hyperandrogenism plays a role in this impaired
286 negative feedback. The opposing effects of androgens and progestins is supported by findings
287 in murine brain slices that androgens interfere with progesterone negative feedback on GnRH

288 neuron firing rate (Pielecka et al., 2006) and GABA transmission to these cells (Sullivan and
289 Moenter, 2005). The elevated LH pulse frequency in PNA mice (Moore et al., 2015) may have a
290 similar origin to that in patients with PCOS. Following ovariectomy, LH levels rise in control mice
291 and to a lesser extent in PNA mice (Moore et al., 2015). Administration of progesterone reduces
292 the LH levels in ovariectomized control but not PNA mice, indicative of impaired negative
293 feedback in the latter (Moore et al., 2015). Progesterone may act in part through receptors in the
294 arcuate nucleus to reduce LH pulse frequency, as administration of progesterone receptor
295 antagonists in this brain region reduces the interval between LH pulses following intraperitoneal
296 injection of progesterone (He et al., 2017). Progesterone also reduces the frequency of peaks in
297 KNDy neuron activity measured by GCaMP fluorescence that are correlated with LH release
298 (McQuillan et al., 2019), but whether or not this is a direct effect on KNDy neurons is not known.

299 A possible alternative mediator of central changes in PNA mice is GABAergic neurons. A subset
300 of KNDy neurons may be GABAergic, though estimates vary on the percentage; up to 50% of
301 KNDy neurons express GAD67 (Cravo et al., 2011), but only about 10-15% of KNDy neurons
302 co-express the vesicular GABA transporter VGaT (Marshall et al., 2017). PNA treatment
303 increases the frequency of GABAergic postsynaptic currents recorded in GnRH neurons from
304 both adult and prepubertal 3wk-old mice (Berg et al., 2018; Sullivan and Moenter, 2004), which
305 given the excitatory effects of GABA in GnRH neurons can contribute to increased activity. At
306 least some of this increased transmission appears to arise from the arcuate nucleus as
307 appositions between GABAergic neurons in the region and GnRH neurons increase in PNA
308 mice (Moore et al., 2015). Consistent with an involvement in the steroid feedback effects
309 discussed above, PNA treatment reduces the expression of progesterone receptors in
310 GABAergic neurons in the arcuate nucleus (Moore et al., 2015). High-frequency optogenetic
311 stimulation of GABAergic neurons in the arcuate can stimulate LH release in control mice (Silva
312 et al., 2019). Longer-term chemogenetic activation of these GABAergic neurons also increases
313 LH release, disrupts estrous cycles and decreases the number of corpora lutea (Silva et al.,
314 2019). Together, these results point to GABAergic neurons in the arcuate as a potential steroid-
315 sensitive mediator of PNA treatment on GnRH activity.

316 It is important to point out that our findings do not rule out a possible role of KNDy neurons in
317 modulating the effects of PNA or age on GnRH and LH release. KNDy neurons are part of an
318 intricate network in the arcuate nucleus, and they project to GnRH distal projections in the
319 median eminence (Yip et al., 2015). In rats, PNA increases the number of arcuate cells
320 immunopositive for kisspeptin and neurokinin B (Osuka et al., 2017) and the relative levels of

321 kisspeptin and neurokinin B mRNA (Yan et al., 2014). In sheep, prenatal testosterone treatment
322 reduced the number of putatively inhibitory dynorphin-immunopositive cells without changing the
323 number of kisspeptin-immunopositive cells in the arcuate nucleus (Cheng et al., 2010). In
324 contrast, following seven days of estradiol treatment, PNA mice did not differ in the relative
325 mRNA expression of KNDy neuron peptides or receptors in the arcuate nucleus (Caldwell et al.,
326 2015). Similarly, we only observed development changes in KNDy neuron peptide and receptor
327 mRNA expression in the arcuate nucleus, but no changes due to PNA treatment. The variation
328 between studies may be attributable to animal models or the examination of mRNA vs peptide.
329 Prenatal testosterone exposure also alters synaptic connections of KNDy neurons with one
330 another and projections to GnRH neurons (Cernea et al., 2015). It remains possible that even
331 without a change in firing frequency, PNA may alter the amount of kisspeptin and/or other
332 neuromodulators released at a given level of activity, potentially leading to increased GnRH
333 release. The reciprocal connections of the network of KNDy neurons are also thought to be
334 important for their involvement in GnRH pulse regulation, and PNA could alter these dynamics.
335 Neurokinin B increases and dynorphin decreases the activity of KNDy neurons (de Croft et al.,
336 2012, 2013; Ruka et al., 2013), whereas kisspeptin does not affect the firing frequency of other
337 KNDy neurons (de Croft et al., 2013). The effects of neurokinin B and dynorphin signaling are
338 modulated by steroidal milieu (Ruka et al., 2016). Intriguingly, in the present study, senktide, a
339 neurokinin-3 receptor agonist, was less effective at eliciting an increase firing frequency of
340 KNDy neurons from 3wk-old PNA mice. This suggests that PNA disrupts the development of
341 this network.

342 A key feature of patients with PCOS is a persistently elevated LH pulse frequency that is most
343 similar to the mid-to-late follicular phase (McCartney et al., 2002). Though we often recorded
344 cells for at least 60min, these recordings were not of sufficient length to characterize rigorously
345 the frequency and duration of peaks and nadirs in firing activity. It is plausible that the firing
346 activity of KNDy neurons during a peak in activity does not differ with age or PNA treatment, but
347 that the frequency of these peaks may be increased in adult PNA mice, leading to the elevated
348 GnRH and LH pulse frequency. In this regard, the frequency of peaks, but not mean firing rate,
349 was altered in KNDy neurons from adult males by orchidectomy and steroid replacement
350 (Vanacker et al., 2017). Because PNA mice fail to exhibit typical estrous cycles and remain
351 persistently in a diestrus-like state based on vaginal cytology, we specifically compared their
352 firing frequency to that of cells from diestrus control mice. The frequency of peaks in calcium
353 activity of KNDy neurons across the estrous cycle was not different from metestrus to diestrus to

354 proestrus (McQuillan et al., 2019). In contrast, KNDy cells from mice in estrus exhibited a
355 markedly decreased frequency of these peaks, postulated to be due in part to the negative
356 feedback effects of progesterone (McQuillan et al., 2019). It is thus possible that a difference in
357 firing rate of KNDy neurons would be observed on estrus that could be attributable to impaired
358 progesterone negative feedback in adult PNA mice. Our choice to record on diestrus was based
359 not only on the practical consideration that PNA mice are often in persistent diestrus, but also
360 on the observed increase in LH pulse frequency in PNA mice during this stage (Moore et al.,
361 2015). The lack of difference in KNDy neuron firing rate in the present study thus supports the
362 postulate that this increased episodic LH release arises from other cells, or is disrupted by the
363 brain slice preparation.

364 The work presented here indicates that the elevated GnRH firing frequency and LH pulse
365 frequency associated with prenatal androgenization cannot be solely explained by changes in
366 arcuate KNDy neuron firing frequency or bursting patterns. PNA may also alter the development
367 of the stimulatory effects of neurokinin B receptor activation on KNDy neuron activity, disrupting
368 network dynamics. Our work points to the importance of the broader network of neurons within
369 the hypothalamus, including GABAergic cells, as mediators of the effects of hyperandrogenism
370 on the output of the hypothalamic-pituitary-gonadal axis.

References

- Abbott, D. H., Rayome, B. H., Dumesic, D. A., Lewis, K. C., Edwards, A. K., Wallen, K., Wilson, M. E., Appt, S. E., & Levine, J. E. (2017). Clustering of PCOS-like traits in naturally hyperandrogenic female rhesus monkeys. *Hum. Reprod.*, *32*(4), 923–936. <https://doi.org/10.1093/humrep/dex036>
- Abbott, D. H., Rogers, J., Dumesic, D. A., & Levine, J. E. (2019). Naturally Occurring and Experimentally Induced Rhesus Macaque Models for Polycystic Ovary Syndrome: Translational Gateways to Clinical Application. *Med. Sci.*, *7*(12), 107. <https://doi.org/10.3390/medsci7120107>
- Abbott, D. H., Barnett, D. K., Levine, J. E., Padmanabhan, V., Dumesic, D. A., Jacoris, S., & Tarantal, A. F. (2008). Endocrine antecedents of polycystic ovary syndrome in fetal and infant prenatally androgenized female rhesus monkeys. *Biol. Reprod.*, *79*(1), 154–163. <https://doi.org/10.1095/biolreprod.108.067702>
- Alcami, P., Franconville, R., Llano, I., & Marty, A. (2012). Measuring the firing rate of high-resistance neurons with cell-attached recording. *J. Neurosci.*, *32*(9), 3118–3130. <https://doi.org/10.1523/JNEUROSCI.5371-11.2012>
- Berg, T., Silveira, M. A., & Moenter, S. M. (2018). Prepubertal Development of GABAergic Transmission to Gonadotropin-Releasing Hormone (GnRH) Neurons and Postsynaptic Response Are Altered by Prenatal Androgenization. *J. Neurosci.*, *38*(9), 2283–2293. <https://doi.org/10.1523/JNEUROSCI.2304-17.2018>
- Birch, R. A., Padmanabhan, V., Foster, D. L., Unsworth, W. P., & Robinson, J. E. (2003). Prenatal programming of reproductive neuroendocrine function: Fetal androgen exposure produces progressive disruption of reproductive cycles in sheep. *Endocrinology*, *144*(4), 1426–1434. <https://doi.org/10.1210/en.2002-220965>
- Bustin, S. (2002). Quantification of mRNA using real-time reverse transcription PCR (RT-PCR): trends and problems. *J. Mol. Endocrinol.*, *29*(1), 23–39. <https://doi.org/10.1677/JME.0.0290023>
- Caldwell, A. S. L., Eid, S., Kay, C. R., Jimenez, M., McMahon, A. C., Desai, R., Allan, C. M., Smith, J. T., Handelsman, D. J., & Walters, K. A. (2015). Haplosufficient Genomic Androgen Receptor Signaling Is Adequate to Protect Female Mice From Induction of Polycystic Ovary Syndrome Features by Prenatal Hyperandrogenization. *Endocrinology*, *156*(4), 1441–1452. <https://doi.org/10.1210/EN.2014-1887>
- Caldwell, A. S. L., Edwards, M. C., Desai, R., Jimenez, M., Gilchrist, R. B., Handelsman, D. J., & Walters, K. A. (2017). Neuroendocrine androgen action is a key extraovarian mediator in the development of polycystic ovary syndrome. *Proc. Natl. Acad. Sci. U. S. A.*, *114*(16), E3334–E3343. <https://doi.org/10.1073/pnas.1616467114>
- Cazalis, M., Dayanithi, G., & Nordmann, J. J. (1985). The role of patterned burst and interburst interval on the excitation-coupling mechanism in the isolated rat neural lobe. *J. Physiol.*, *369*, 45–60. <http://www.ncbi.nlm.nih.gov/pubmed/4093889>

- Cernea, M., Padmanabhan, V., Goodman, R. L., Coolen, L. M., & Lehman, M. N. (2015). Prenatal testosterone treatment leads to changes in the morphology of KNDy neurons, their inputs, and projections to GnRH cells in female sheep. *Endocrinology*, *156*(9), 3277–3291. <https://doi.org/10.1210/en.2014-1609>
- Chang, W. (2014). *extrafont: Tools for using fonts* (R package version 0.17). <https://cran.r-project.org/package=extrafont>
- Chang, W., Cheng, J., Allaire, J., Xie, Y., & McPherson, J. (2020). *shiny: Web Application Framework for R* (R package version 1.5.0). <https://cran.r-project.org/package=shiny>
- Cheng, G., Coolen, L. M., Padmanabhan, V., Goodman, R. L., & Lehman, M. N. (2010). The kisspeptin/neurokinin B/dynorphin (KNDy) cell population of the arcuate nucleus: Sex differences and effects of prenatal testosterone in sheep. *Endocrinology*, *151*(1), 301–311. <https://doi.org/10.1210/en.2009-0541>
- Clarkson, J., Han, S. Y., Piet, R., McLennan, T., Kane, G. M., Ng, J., Porteous, R. W., Kim, J. S., Colledge, W. H., Iremonger, K. J., & Herbison, A. E. (2017). Definition of the hypothalamic GnRH pulse generator in mice. *Proc. Natl. Acad. Sci. U. S. A.*, *114*(47), E10216–E10223. <https://doi.org/10.1073/pnas.1713897114>
- Cravo, R. M., Margatho, L. O., Osborne-Lawrence, S., Donato, J., Atkin, S., Bookout, A. L., Rovinsky, S., Frazão, R., Lee, C. E., Gautron, L., Zigman, J. M., & Elias, C. F. (2011). Characterization of Kiss1 neurons using transgenic mouse models. *Neuroscience*, *173*, 37–56. <https://doi.org/10.1016/j.neuroscience.2010.11.022>
- de Croft, S., Piet, R., Mayer, C., Mai, O., Boehm, U., & Herbison, A. E. (2012). Spontaneous Kisspeptin Neuron Firing in the Adult Mouse Reveals Marked Sex and Brain Region Differences but No Support for a Direct Role in Negative Feedback. *Endocrinology*, *153*(11), 5384–5393. <https://doi.org/10.1210/en.2012-1616>
- de Croft, S., Boehm, U., & Herbison, A. E. (2013). Neurokinin B Activates Arcuate Kisspeptin Neurons Through Multiple Tachykinin Receptors in the Male Mouse. *Endocrinology*, *154*(8), 2750–2760. <https://doi.org/10.1210/en.2013-1231>
- Dulka, E. A., & Moenter, S. M. (2017). Prepubertal development of gonadotropin-releasing hormone neuron activity is altered by sex, age, and prenatal androgen exposure. *Endocrinology*, *158*(11), 3943–3953. <https://doi.org/10.1210/en.2017-00768>
- Dumesic, D. A., Abbott, D. H., Eisner, J. R., & Goy, R. W. (1997). Prenatal exposure of female rhesus monkeys to testosterone propionate increases serum luteinizing hormone levels in adulthood. *Fertil. Steril.*, *67*(1), 155–163. [https://doi.org/10.1016/S0015-0282\(97\)81873-0](https://doi.org/10.1016/S0015-0282(97)81873-0)
- Dumesic, D. A., Oberfield, S. E., Stener-Victorin, E., Marshall, J. C., Laven, J. S., & Legro, R. S. (2015). Scientific statement on the diagnostic criteria, epidemiology, pathophysiology, and molecular genetics of polycystic ovary syndrome. In *Endocrine Reviews* (Vol. 36, Issue 5, pp. 487–525). Endocrine Society. <https://doi.org/10.1210/er.2015-1018>
- Dutton, A., & Dyball, R. E. (1979). Phasic firing enhances vasopressin release from the rat

neurohypophysis. *J. Physiol.*, 290(2), 433–440.
<http://www.ncbi.nlm.nih.gov/pubmed/469785>

Eagleson, C. A., Gingrich, M. B., Pastor, C. L., Arora, T. K., Burt, C. M., Evans, W. S., & Marshall, J. C. (2000). Polycystic Ovarian Syndrome: Evidence that Flutamide Restores Sensitivity of the Gonadotropin-Releasing Hormone Pulse Generator to Inhibition by Estradiol and Progesterone. *J. Clin. Endocrinol. Metab.*, 85(11), 4047–4052.
<https://doi.org/10.1210/jcem.85.11.6992>

Foeking, E. M., Szabo, M., Schwartz, N. B., & Levine, J. E. (2005). Neuroendocrine consequences of prenatal androgen exposure in the female rat: Absence of luteinizing hormone surges, suppression of progesterone receptor gene expression, and acceleration of the gonadotropin-releasing hormone pulse generator. *Biol. Reprod.*, 72(6), 1475–1483.
<https://doi.org/10.1095/biolreprod.105.039800>

Fox, J., & Weisberg, S. (2019). *An {R} Companion to Applied Regression* (Third). Sage.
<https://socialsciences.mcmaster.ca/jfox/Books/Companion/>

Frazao, R., Cravo, R. M., Donato, J., Ratra, D. V., Clegg, D. J., Elmquist, J. K., Zigman, J. M., Williams, K. W., & Elias, C. F. (2013). Shift in Kiss1 Cell Activity Requires Estrogen Receptor α . *J. Neurosci.*, 33(7), 2807–2820. <https://doi.org/10.1523/JNEUROSCI.1610-12.2013>

Glanowska, K. M., Burger, L. L., & Moenter, S. M. (2014). Development of Gonadotropin-Releasing Hormone Secretion and Pituitary Response. *J. Neurosci.*, 34(45), 15060–15069.
<https://doi.org/10.1523/JNEUROSCI.2200-14.2014>

Gohel, D. (2020a). *flextable: Functions for Tabular Reporting* (R package version 0.5.11).
<https://cran.r-project.org/package=flextable>

Gohel, D. (2020b). *officer: Manipulation of Microsoft Word and PowerPoint Documents* (R package version 0.3.15). <https://cran.r-project.org/package=officer>

Haisenleder, D. J., Dalkin, A. C., Ortolano, G. A., Marshall, J. C., & Shupnik, M. A. (1991). A pulsatile gonadotropin-releasing hormone stimulus is required to increase transcription of the gonadotropin subunit genes: Evidence for differential regulation of transcription by pulse frequency in vivo. *Endocrinology*, 128(1), 509–517. <https://doi.org/10.1210/endo-128-1-509>

Han, S.-K., Gottsch, M. L., Lee, K. J., Popa, S. M., Smith, J. T., Jakawich, S. K., Clifton, D. K., Steiner, R. A., & Herbison, A. E. (2005). Activation of Gonadotropin-Releasing Hormone Neurons by Kisspeptin as a Neuroendocrine Switch for the Onset of Puberty. *J. Neurosci.*, 25(49), 11349–11356. <https://doi.org/10.1523/JNEUROSCI.3328-05.2005>

Han, S. Y., McLennan, T., Czielesky, K., & Herbison, A. E. (2015). Selective optogenetic activation of arcuate kisspeptin neurons generates pulsatile luteinizing hormone secretion. *Proc. Natl. Acad. Sci. U. S. A.*, 112(42), 13109–13114.
<https://doi.org/10.1073/pnas.1512243112>

- He, W., Li, X., Adekunbi, D., Liu, Y., Long, H., Wang, L., Lyu, Q., Kuang, Y., & O'Byrne, K. T. (2017). Hypothalamic effects of progesterone on regulation of the pulsatile and surge release of luteinising hormone in female rats. *Sci. Rep.*, *7*(1), 1–11. <https://doi.org/10.1038/s41598-017-08805-1>
- Henry, L., & Wickham, H. (2020a). *purrr: Functional Programming Tools* (R package version 0.3.4). <https://cran.r-project.org/package=purrr>
- Henry, L., & Wickham, H. (2020b). *rlang: Functions for Base Types and Core R and “Tidyverse” Features* (R package version 0.4.8). <https://cran.r-project.org/package=rlang>
- Herbison, A. E., Skinner, D. C., Robinson, J. E., & King, I. S. (1996). Androgen receptor-Immunoreactive cells in ram hypothalamus: Distribution and co-localization patterns with gonadotropin-releasing hormone, somatostatin and tyrosine hydroxylase. *Neuroendocrinology*, *63*(2), 120–131. <https://doi.org/10.1159/000126948>
- Kassambara, A. (2020). *ggpubr: “ggplot2” Based Publication Ready Plots* (R package version 0.4.0). <https://cran.r-project.org/package=ggpubr>
- Kassambara, A. (2021). *rstatix: Pipe-Friendly Framework for Basic Statistical Tests* (R package version 0.7.0). <https://cran.r-project.org/package=rstatix>
- Levine, J. E., & Ramirez, V. D. (1982). Luteinizing hormone-releasing hormone release during the rat estrous cycle and after ovariectomy, as estimated with push-pull cannulae. *Endocrinology*, *111*(5), 1439–1448. <https://doi.org/10.1210/endo-111-5-1439>
- Marshall, C. J., Desroziere, E., McLennan, T., & Campbell, R. E. (2017). Defining Subpopulations of Arcuate Nucleus GABA Neurons in Male, Female, and Prenatally Androgenized Female Mice. *Neuroendocrinology*, *105*(2), 157–169. <https://doi.org/10.1159/000452105>
- McCartney, C. R., Eagleson, C. A., & Marshall, J. C. (2002). Regulation of Gonadotropin Secretion: Implications for Polycystic Ovary Syndrome. *Semin. Reprod. Med.*, *20*(4), 317–326. <https://doi.org/10.1055/s-2002-36706>
- McQuillan, H. J., Han, S. Y., Cheong, I., & Herbison, A. E. (2019). GnRH Pulse Generator Activity Across the Estrous Cycle of Female Mice. *Endocrinology*, *160*, 1480–1491. <https://doi.org/10.1210/en.2019-00193>
- Messenger, S., Chatzidaki, E. E., Ma, D., Hendrick, A. G., Zahn, D., Dixon, J., Thresher, R. R., Malinge, I., Lomet, D., Carlton, M. B. L., Colledge, W. H., Caraty, A., & Aparicio, S. A. J. R. (2005). Kisspeptin directly stimulates gonadotropin-releasing hormone release via G protein-coupled receptor 54. *Proc. Natl. Acad. Sci. U. S. A.*, *102*(5), 1761–1766. <https://doi.org/10.1073/pnas.0409330102>
- Moenter, S. M., Caraty, A., Locatelli, A., & Karsch, F. J. (1991). Pattern of Gonadotropin-Releasing Hormone (GnRH) Secretion Leading up to Ovulation in the Ewe: Existence of a Preovulatory GnRH Surge. *Endocrinology*, *129*(3), 1175–1182. <https://doi.org/10.1210/endo-129-3-1175>

- Moore, A. M., Prescott, M., Marshall, C. J., Yip, S. H., & Campbell, R. E. (2015). Enhancement of a robust arcuate GABAergic input to gonadotropin-releasing hormone neurons in a model of polycystic ovarian syndrome. *Proc. Natl. Acad. Sci.*, *112*(2), 596–601. <https://doi.org/10.1073/pnas.1415038112>
- Nunemaker, C. S., DeFazio, R. A., & Moenter, S. M. (2003). A targeted extracellular approach for recording long-term firing patterns of excitable cells: a practical guide. *Biol. Proced. Online*, *5*(1), 53–62. <https://doi.org/10.1251/bpo46>
- Oakley, A. E., Clifton, D. K., & Steiner, R. A. (2009). Kisspeptin signaling in the brain. *Endocr. Rev.*, *30*(6), 713–743. <https://doi.org/10.1210/er.2009-0005>
- Osuka, S., Iwase, A., Nakahara, T., Kondo, M., Saito, A., Nakamura, T., Takikawa, S., Goto, M., Kotani, T., & Kikkawa, F. (2017). Kisspeptin in the Hypothalamus of 2 Rat Models of Polycystic Ovary Syndrome. *Endocrinology*, *158*(2), 367–377. <https://doi.org/10.1210/en.2016-1333>
- Pastor, C. L., Griffin-Korf, M. L., Aloji, J. A., Evans, W. S., & Marshall, J. C. (1998). Polycystic Ovary Syndrome: Evidence for Reduced Sensitivity of the Gonadotropin-Releasing Hormone Pulse Generator to Inhibition by Estradiol and Progesterone. *J. Clin. Endocrinol. Metab.*, *83*(2), 582–590. <https://doi.org/10.1210/jcem.83.2.4604>
- Pielecka-Fortuna, J., Chu, Z., & Moenter, S. M. (2008). Kisspeptin Acts Directly and Indirectly to Increase Gonadotropin-Releasing Hormone Neuron Activity and Its Effects Are Modulated by Estradiol. *Endocrinology*, *149*(4), 1979–1986. <https://doi.org/10.1210/en.2007-1365>
- Pielecka, J., Quaynor, S. D., & Moenter, S. M. (2006). Androgens increase gonadotropin-releasing hormone neuron firing activity in females and interfere with progesterone negative feedback. *Endocrinology*, *147*(3), 1474–1479. <https://doi.org/10.1210/en.2005-1029>
- R Core Team. (2019). *R: A language and environment for statistical computing*. R Foundation for Statistical Computing. <https://www.r-project.org/>
- Roland, A. V., & Moenter, S. M. (2011). Prenatal androgenization of female mice programs an increase in firing activity of gonadotropin-releasing hormone (GnRH) neurons that is reversed by metformin treatment in adulthood. *Endocrinology*, *152*(2), 618–628. <https://doi.org/10.1210/en.2010-0823>
- Rosenfield, R. L. (2007). Identifying Children at Risk for Polycystic Ovary Syndrome. *J. Clin. Endocrinol. Metab.*, *92*(3), 787–796. <https://doi.org/10.1210/jc.2006-2012>
- RStudio Team. (2019). *RStudio: Integrated Development Environment for R*. <http://www.rstudio.com/>
- Ruka, K. A., Burger, L. L., & Moenter, S. M. (2013). Regulation of Arcuate Neurons Coexpressing Kisspeptin, Neurokinin B, and Dynorphin by Modulators of Neurokinin 3 and κ -Opioid Receptors in Adult Male Mice. *Endocrinology*, *154*(8), 2761–2771. <https://doi.org/10.1210/en.2013-1268>

- Ruka, K. A., Burger, L. L., & Moenter, S. M. (2016). Both estrogen and androgen modify the response to activation of neurokinin-3 and κ -opioid receptors in arcuate kisspeptin neurons from male mice. *Endocrinology*, *157*(2), 752–763. <https://doi.org/10.1210/en.2015-1688>
- Schauberger, P., & Walker, A. (2020). *openxlsx: Read, Write and Edit xlsx Files* (R package version 4.2.3). <https://cran.r-project.org/package=openxlsx>
- Schloerke, B., Cook, D., Larmarange, J., Briatte, F., Marbach, M., Thoen, E., Elberg, A., & Crowley, J. (2020). *GGally: Extension to “ggplot2”* (R package version 2.0.0). <https://cran.r-project.org/package=GGally>
- Silva, M. S. B., Desroziers, E., Hessler, S., Prescott, M., Coyle, C., Herbison, A. E., & Campbell, R. E. (2019). Activation of arcuate nucleus GABA neurons promotes luteinizing hormone secretion and reproductive dysfunction: Implications for polycystic ovary syndrome. *EBioMedicine*, *44*, 582–596. <https://doi.org/10.1016/J.EBIOM.2019.05.065>
- Simonoff, J. S. (2003). Multidimensional Contingency Tables. In *Analyzing Categorical Data. Springer Texts in Statistics*. (pp. 309–364). Springer. https://doi.org/10.1007/978-0-387-21727-7_8
- Smith, J. T., Dungan, H. M., Stoll, E. A., Gottsch, M. L., Braun, R. E., Eacker, S. M., Clifton, D. K., & Steiner, R. A. (2005). Differential Regulation of KiSS-1 mRNA Expression by Sex Steroids in the Brain of the Male Mouse. *Endocrinology*, *146*(7), 2976–2984. <https://doi.org/10.1210/en.2005-0323>
- Sullivan, S. D., & Moenter, S. M. (2004). Prenatal androgens alter GABAergic drive to gonadotropin-releasing hormone neurons: Implications for a common fertility disorder. *Proc. Natl. Acad. Sci.*, *101*(18), 7129–7134. <https://doi.org/10.1073/pnas.0308058101>
- Sullivan, S. D., & Moenter, S. M. (2005). GABAergic integration of progesterone and androgen feedback to gonadotropin-releasing hormone neurons. *Biol. Reprod.*, *72*(1), 33–41. <https://doi.org/10.1095/biolreprod.104.033126>
- Underwood, A. J. (1997). *Experiments in Ecology: Their Logical Design and Interpretation Using Analysis of Variance*. Cambridge University Press.
- Vanacker, C., Moya, M. R., DeFazio, R. A., Johnson, M. L., & Moenter, S. M. (2017). Long-Term Recordings of Arcuate Nucleus Kisspeptin Neurons Reveal Patterned Activity That Is Modulated by Gonadal Steroids in Male Mice. *Endocrinology*, *158*(10), 3553–3564. <https://doi.org/10.1210/en.2017-00382>
- Veiga-Lopez, A., Ye, W., Phillips, D. J., Herkimer, C., Knight, P. G., & Padmanabhan, V. (2008). Developmental programming: Deficits in reproductive hormone dynamics and ovulatory outcomes in prenatal, testosterone-treated sheep. *Biol. Reprod.*, *78*(4), 636–647. <https://doi.org/10.1095/biolreprod.107.065904>
- Walters, K. A., Edwards, M. C., Tesic, D., Caldwell, A. S. L., Jimenez, M., Smith, J. T., & Handelsman, D. J. (2018). The Role of Central Androgen Receptor Actions in Regulating the Hypothalamic-Pituitary-Ovarian Axis. *Neuroendocrinology*, *106*(4), 389–400.

<https://doi.org/10.1159/000487762>

Wickham, H., & Hester, J. (2020). *readr: Read Rectangular Text Data* (R package version 1.4.0). <https://cran.r-project.org/package=readr>

Wickham, H., François, R., Henry, L., & Müller, K. (2020). *dplyr: A Grammar of Data Manipulation* (R package version 1.0.2). <https://cran.r-project.org/package=dplyr>

Wickham, H., & Seidel, D. (2020). *scales: Scale Functions for Visualization* (R package version 1.1.1). <https://cran.r-project.org/package=scales>

Wickham, H. et al. (2019). Welcome to the Tidyverse. *J. Open Source Softw.*, 4(43), 1686. <https://doi.org/10.21105/joss.01686>

Wildt, L., Hausler, A., Marshall, G., Hutchison, J. S., Plant, T. M., Belchetz, P. E., & Knobil, E. (1981). Frequency and amplitude of gonadotropin-releasing hormone stimulation and gonadotropin secretion in the rhesus monkey. *Endocrinology*, 109(2), 376–385. <https://doi.org/10.1210/endo-109-2-376>

Wilke, C. O. (2020). *cowplot: Streamlined Plot Theme and Plot Annotations for “ggplot2”* (R package version 1.1.1.). <https://cran.r-project.org/package=cowplot>

Xie, Y. (2014). knitr: A Comprehensive Tool for Reproducible Research in R. In V. Stodden, F. Leisch, & R. D. Peng (Eds.), *Implementing Reproducible Research*. Chapman and Hall/CRC. <https://doi.org/10.1201/9781315373461-1>

Xie, Y. (2015). *Dynamic Documents with R and knitr* (2nd ed.). Chapman and Hall/CRC.

Xie, Y. (2020). *knitr: A General-Purpose Package for Dynamic Report Generation in R*. <https://yihui.org/knitr/>

Xie, Y., Cheng, J., & Tan, X. (2021). *DT: A Wrapper of the JavaScript Library “DataTables”* (R package version 0.18). <https://cran.r-project.org/package=DT>

Yan, X., Yuan, C., Zhao, N., Cui, Y., & Liu, J. (2014). Prenatal androgen excess enhances stimulation of the GNRH pulse in pubertal female rats. *J. Endocrinol.*, 222(1), 73–85. <https://doi.org/10.1530/JOE-14-0021>

Yip, S. H., Boehm, U., Herbison, A. E., & Campbell, R. E. (2015). Conditional Viral Tract Tracing Delineates the Projections of the Distinct Kisspeptin Neuron Populations to Gonadotropin-Releasing Hormone (GnRH) Neurons in the Mouse. *Endocrinology*, 156(7), 2582–2594. <https://doi.org/10.1210/en.2015-1131>

Zhu, H. (2020). *kableExtra: Construct Complex Table with “kable” and Pipe Syntax* (R package version 1.3.1). <https://cran.r-project.org/package=kableExtra>

Tables

Table 1 Probes and primers sequences for PCR experiments (Figure 5).

Transcript	Probe 5'→3'	Forward 5'→3'	Reverse 5'→3'
<i>Actb</i>	CTG GCC TCA CTG TCC ACC TTC C	GAT TAC TGC TCT GGC TCC TAG	GAC TCA TCG TAC TCC TGC TTG
<i>Syn1</i>	ACG TGT CTA CCC ACA ACT TGT ACC TG	CTT GAG CAG ATT GCC ATG TC	ACC TCA ATA ATG TGA TCC CTT CC
<i>Kiss1</i>	CGG ACT GCT GGC CTG TGG AT	CTG CTT CTC CTC TGT GTC G	TTC CCA GGC ATT AAC GAG TTC
<i>Kiss1r</i>	TCA ATC CGC TGC TCT ATG CCT TCC	CTC ACT GCA TGT CCT ACA GC	GCC TGT CTG AAG TGT GAA CC
<i>Tac2</i>	AGC TTT GTC CTT CAG GCA CCA TGA	CTG CAC TCT TGT CTC TGT CT	ACA GCC GCA AAC AGC AT
<i>Tacr3</i>	TCT CTT GAA GCC TGC ACG AAA TCT TTT G	AGC TCA ACC ATG TAC AAC CC	CTC ATC GTA GCT GGA GAC TTG
<i>Pdyn</i>	TCA ACC CCC TGA TTT GCT CCC TG	GTG CAG TGA GGA TTC AGG ATG	CAT GTC TCC CAC TCC TCT GA
<i>Opkr1</i>	AGA GAA TTG CCC ACT AAG CCC ACC	CAT CAC CGC TGT CTA CTC TG	GGT CTT CAT CTT CGT GTA TCG G
<i>Ar</i>	ACC ACA TGC ACA AGC TGC CTC T	CTG CCT TGT TAT CTA GCC TCA	ATA CTG AAT GAC CGC CAT CTG
<i>Esr1</i>	TGC CTT CCA CAC ATT TAC CTT GAT TCC T	CCT GTT TGC TCC TAA CTT GCT	GAA CCG ACT TGA CGT AGC C
<i>Pgr</i>	AGA TTC AGA AGC CAG CCA GAG CC	CGC CAT ACC TTA ACT ACC TGA G	CCA TAG TGA CAG CCA GAT GC

Table 2 Statistical parameters characterizing the PNA phenotype (Figure 1). Bold indicates $p < 0.05$. Std resid, standardized residuals of PNA group from Chi-square test

Property	Two-tailed unpaired Welch-corrected Student's <i>t</i> -test	Mean Difference		Effect Size – Cohen's <i>d</i>	
Anogenital Distance (mm)	$t_{30.13} = 10.052$, $p < 0.0001$	Diff 2.06 [CI 1.64, 2.48]		$d = 3.03$	
Body mass (g)	$t_{32.03} = 2.331$, $p = 0.0262$	Diff 2.26 [CI 0.29, 4.24]		$d = 0.707$	
Property	Chi-square test		Estrus	Diestrus	Proestrus
Estrous cycle stage distribution	$\chi^2 = 111.392$, $n = 992$, $df = 2$, $p < 0.0001$	Std resid:	-1.79	7.08	10.11
		Fisher's exact test; Bonferroni adjusted:	$p = 0.226$	$p < 0.0001$	$p < 0.0001$

Table 3. Statistical parameters for firing activity (Figure 2). Independence of treatment and age with firing proportion was assessed with Breslow-Day test. This was followed by the Mantel-Haenszel Chi-squared test with continuity correction to determine the effect of treatment on firing proportion when controlling for age (Simonoff, 2003). A two-way ANOVA was conducted for firing frequency.

Parameter	<i>Breslow-Day test for independence</i>		<i>Mantel-Haenszel Chi-squared</i>
Proportion firing	$\chi^2 = 1.285, df = 1, p = 0.257$		$\chi^2 = 0.069, df = 1, p\text{-value} = 0.7932$
Parameter	<i>age</i>	<i>PNA treatment</i>	<i>interaction</i>
firing frequency	Diff -0.193 [CI -0.537, 0.151]	Diff -0.104 [CI -0.448, 0.240]	Diff 0.130 [CI -0.558, 0.819]
	$F(1, 66) = 1.251;$ $p = 0.267$	$F(1, 66) = 0.362;$ $p = 0.549$	$F(1, 66) = 0.143;$ $p = 0.707$

Table 4. Statistical parameters from three-way mixed model ANOVA assessing the effect of age and PNA treatment on the KNDy cell response to senktide (Figure 3). The effect size, generalized η^2 , is reported for each effect. Bonferroni multiple comparisons for cells that differ by only one factor. Bold indicates $p < 0.05$.

Effect	Statistic	generalized η^2
senktide	$F(1, 38) = 52.35, p < 0.0001$	0.395
age	$F(1, 38) = 0.7515, p = 0.391$	0.010
PNA treatment	$F(1, 38) = 2.235, p = 0.143$	0.030
senktide x age	$F(1, 38) = 0.5459, p = 0.465$	0.007
senktide x PNA treatment	$F(1, 38) = 2.051, p = 0.160$	0.025
age x treatment	$F(1, 38) = 0.2633, p = 0.611$	0.004
senktide x age x PNA treatment	$F(1, 38) = 1.179, p = 0.284$	0.015
Bonferroni's multiple comparisons test	<i>Mean diff (Hz), 95% CI of diff</i>	<i>Statistic</i>
SK 3wk-CON – C 3wk-CON	Diff 2.36, [CI 0.59, 4.13]	$t_{38} = 4.055, p = \mathbf{0.003}$
SK 3wk-PNA – C 3wk-PNA	Diff 1.04, [CI -0.41, 2.49]	$t_{38} = 2.192, p = 0.415$
SK adult-CON – C adult-CON	Diff 2.178, [CI 0.40, 3.95]	$t_{38} = 3.743, p = \mathbf{0.007}$
SK adult-PNA – C adult-PNA	Diff 2.00, [CI 0.66, 3.34]	$t_{38} = 4.540, p = \mathbf{0.001}$
C 3wk-PNA – C 3wk-CON	Diff 0.11, [CI -1.51, 1.72]	$t_{76} = 0.194, p > 0.999$
C adult-PNA – C adult-CON	Diff -0.18, [CI -1.75, 1.39]	$t_{76} = 0.340, p > 0.999$
SK 3wk-PNA – SK 3wk-CON	Diff -1.21, [CI -2.82, 0.40]	$t_{76} = 2.223, p = 0.350$
SK adult-PNA – SK adult-CON	Diff -0.36, [CI -1.93, 1.20]	$t_{76} = 0.682, p > 0.999$
C adult-CON – C 3wk-CON	Diff 0.19, [CI -1.58, 1.95]	$t_{76} = 0.315, p > 0.999$
C adult-PNA – C 3wk-PNA	Diff -0.10, [CI -1.49, 1.29]	$t_{76} = 0.207, p > 0.999$
SK adult-CON – SK 3wk-CON	Diff 0.01, [CI -1.76, 1.77]	$t_{76} = 0.011, p > 0.999$
SK adult-PNA – SK 3wk-PNA	Diff 0.86, CI [-0.53, 2.25]	$t_{76} = 1.825, p = 0.863$

Table 5. Two-way ANOVA statistical parameters for burst parameters. Bold indicates $p < 0.05$.

Property	age	PNA treatment	interaction
burst frequency	Diff -0.030 [CI -0.086, 0.025]	Diff -0.014 [CI -0.070, 0.041]	Diff 0.023 [CI -0.088, 0.134]
	$F(1, 66) = 1.184$; $p = 0.281$	$F(1, 66) = 0.267$; $p = 0.608$	$F(1, 66) = 0.167$; $p = 0.684$
burst duration	Diff 0.116 [CI 0.011, 0.221]	Diff 0.063 [CI -0.042, 0.168]	Diff 0.116 [CI -0.94, 0.326]
	$F(1, 35) = 5.068$; $p = 0.031$	$F(1, 35) = 1.479$; $p = 0.232$	$F(1, 35) = 1.263$; $p = 0.269$
spikes per burst	Diff 0.954 [CI -0.178, 2.087]	Diff 0.560 [CI -0.572, 1.693]	Diff 0.955 [CI -1.310, 3.220]
	$F(1, 35) = 2.927$; $p = 0.096$	$F(1, 35) = 1.009$; $p = 0.322$	$F(1, 35) = 0.733$; $p = 0.398$
intra-burst interval	Diff 0.002 [CI -0.039, 0.044]	Diff 0.021 [CI -0.021, 0.062]	Diff -0.003 [CI -0.085, 0.079]
	$F(1, 35) = 0.013$; $p = 0.911$	$F(1, 35) = 1.021$; $p = 0.319$	$F(1, 35) = 0.005$; $p = 0.942$
single spike frequency	Diff -0.073 [CI -0.187, 0.041]	Diff -0.015 [CI -0.129, 0.099]	Diff -0.122 [CI -0.350, 0.106]
	$F(1, 66) = 1.63$; $p = 0.206$	$F(1, 66) = 0.072$; $p = 0.790$	$F(1, 66) = 1.147$; $p = 0.288$
interburst interval	Diff -14.87 [CI -84.09, 54.36]	Diff 13.72 [CI -55.51, 82.94]	Diff 87.73 [CI -50.71, 226.2]
	$F(1, 42) = 0.188$; $p = 0.667$	$F(1, 42) = 0.160$; $p = 0.691$	$F(1, 42) = 1.635$; $p = 0.208$

Table 6. Two-way ANOVA statistical parameters for arcuate mRNA expression. Bold indicates $p < 0.05$.

Transcript	age	PNA treatment	interaction
<i>Actb</i>	Diff -0.018 [CI -0.074, 0.038]	Diff -0.019 [CI -0.074, 0.037]	Diff -0.019 [CI -0.131, 0.092]
	$F(1, 28) = 0.436$; $p = 0.515$	$F(1, 28) = 0.466$; $p = 0.501$	$F(1, 28) = 0.126$; $p = 0.725$
<i>Syn1</i>	Diff 0.018 [CI -0.038, 0.074]	Diff 0.019 [CI -0.037, 0.074]	Diff 0.019 [CI -0.092, 0.131]
	$F(1, 28) = 0.436$; $p = 0.515$	$F(1, 28) = 0.466$; $p = 0.501$	$F(1, 28) = 0.126$; $p = 0.725$
<i>Kiss1</i>	Diff 0.068 [CI -0.358, 0.495]	Diff 0.019 [CI -0.407, 0.445]	Diff 0.028 [CI -0.824, 0.880]
	$F(1, 28) = 0.108$; $p = 0.744$	$F(1, 28) = 0.009$; $p = 0.926$	$F(1, 28) = 0.004$; $p = 0.947$
<i>Kiss1r</i>	Diff -0.019 [CI -0.170, 0.132]	Diff 0.129 [CI -0.022, 0.280]	Diff 0.150 [CI -0.152, 0.453]
	$F(1, 28) = 0.068$; $p = 0.796$	$F(1, 28) = 3.062$; $p = 0.091$	$F(1, 28) = 1.038$; $p = 0.317$
<i>Tac2</i>	Diff 1.075 [CI 0.584, 1.566]	Diff 0.009 [CI -0.482, 0.500]	Diff 0.264 [CI -0.718, 1.245]
	$F(1, 28) = 20.113$; $p = 0.0001$	$F(1, 28) = 0.001$; $p = 0.97$	$F(1, 28) = 0.302$; $p = 0.587$
<i>Tacr3</i>	Diff 1.064 [CI 0.707, 1.420]	Diff 0.108 [CI -0.249, 0.464]	Diff -0.476 [CI -1.189, 0.238]
	$F(1, 28) = 37.321$; $p < 0.0001$	$F(1, 28) = 0.381$; $p = 0.542$	$F(1, 28) = 1.865$; $p = 0.183$
<i>Pdyn</i>	Diff 0.138 [CI -0.224, 0.499]	Diff 0.331 [CI -0.030, 0.693]	Diff -0.153 [CI -0.876, 0.571]
	$F(1, 28) = 0.608$; $p = 0.442$	$F(1, 28) = 3.520$; $p = 0.071$	$F(1, 28) = 0.187$; $p = 0.669$
<i>Opkr1</i>	Diff 0.127 [CI -0.044, 0.298]	Diff 0.095 [CI -0.076, 0.266]	Diff -0.170 [CI -0.512, 0.172]
	$F(1, 28) = 2.313$; $p = 0.139$	$F(1, 28) = 1.294$; $p = 0.265$	$F(1, 28) = 1.033$; $p = 0.318$
<i>Ar</i>	Diff 0.673 [CI 0.493, 0.854]	Diff 0.041 [CI -0.140, 0.221]	Diff 0.150 [CI -0.212, 0.511]
	$F(1, 28) = 58.323$; $p < 0.0001$	$F(1, 28) = 0.215$; $p = 0.647$	$F(1, 28) = 0.720$; $p = 0.403$
<i>Esr1</i>	Diff 0.091 [CI -0.195, 0.377]	Diff 0.002 [CI -0.284, 0.288]	Diff -0.105 [CI -0.677, 0.467]
	$F(1, 28) = 0.428$; $p = 0.519$	$F(1, 28) = 0.0002$; $p = 0.989$	$F(1, 28) = 0.141$; $p = 0.71$
<i>Pgr</i>	Diff 0.955 [CI 0.585, 1.325]	Diff -0.114 [CI -0.484, 0.257]	Diff 0.076 [CI -0.664, 0.817]
	$F(1, 28) = 27.92$; $p < 0.0001$	$F(1, 28) = 0.395$; $p = 0.535$	$F(1, 28) = 0.045$; $p = 0.834$

Figures and legends

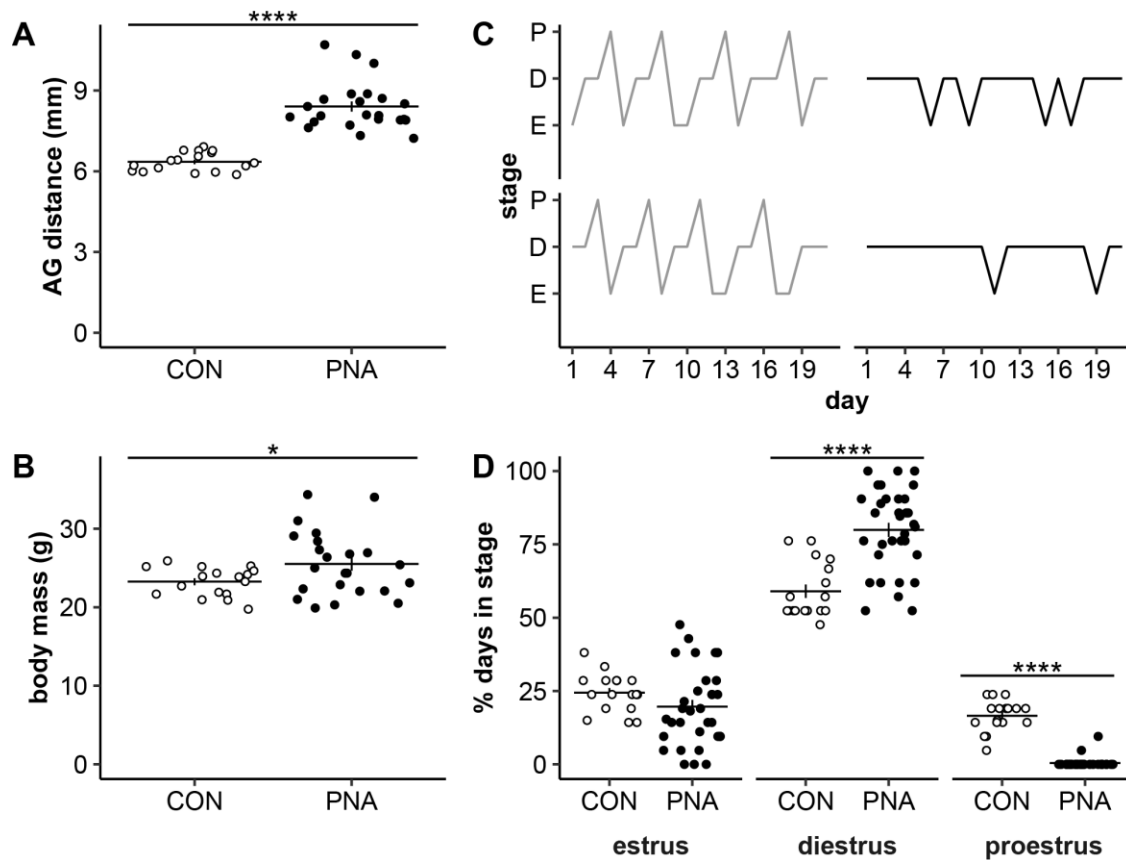


Figure 1. Confirmation of PNA phenotype in adults and surviving littermates of 3wk mice used for electrophysiology. A, B, D. Individual values (CON open symbols, PNA black symbols) and mean \pm SEM anogenital (AG) distance (A), body mass (B) or percent days in each cycle stage (D). C. Representative estrous cycles over a 3-week period; P proestrus, D diestrus, E estrus. Statistical parameters reported in Table 2. * $p < 0.05$, **** $p \leq 0.0001$

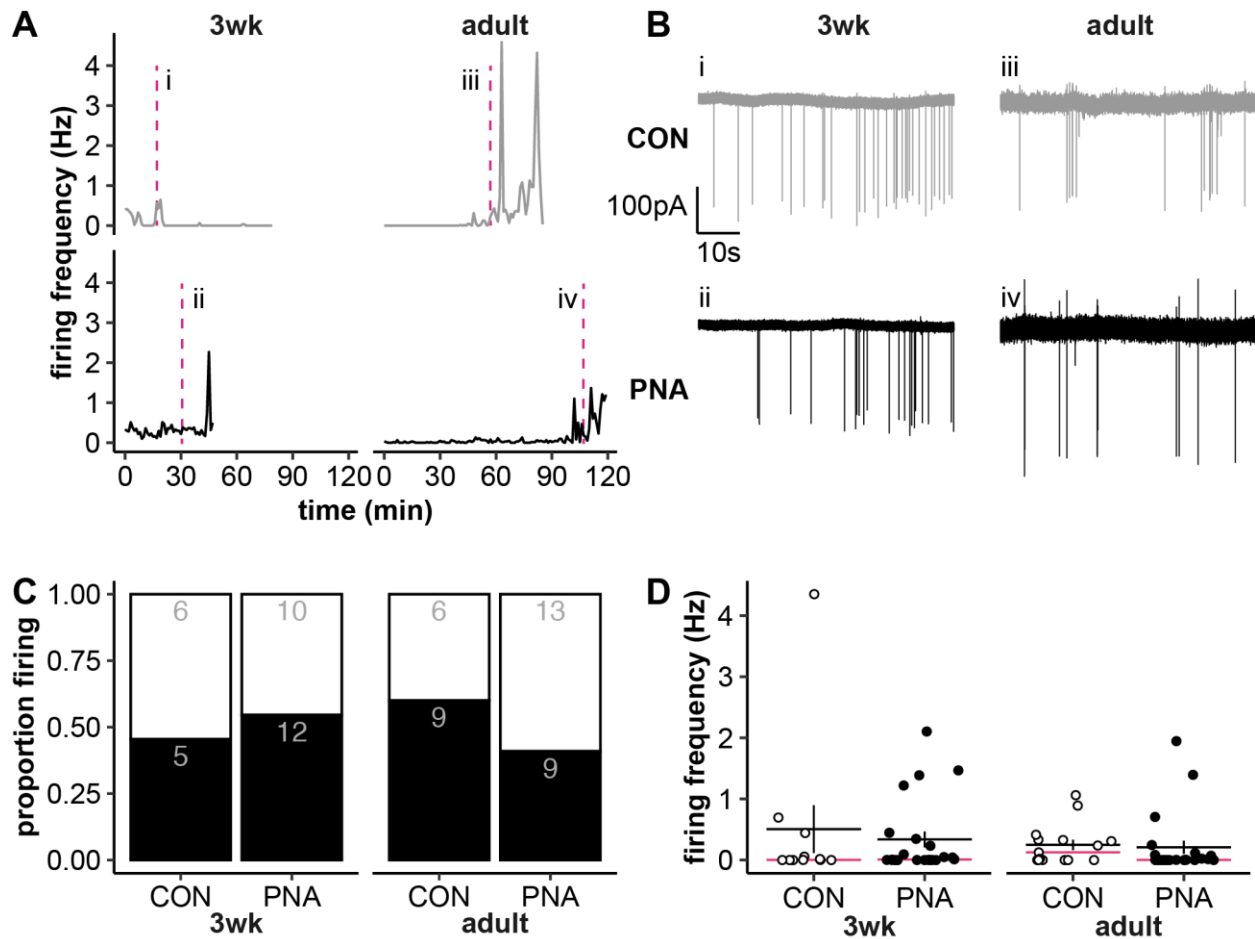


Figure 2. Effect of age and PNA treatment on KNDy neuron firing activity. A, Representative long-term firing patterns (1-min bins). CON are shown on the top in grey, PNA on the bottom in black for each age. The time of the traces shown in B is designated by the magenta dashed lines in panel A. B, Examples of raw firing data (60s) from the areas indicated in A, details as in A. The selected 60s bins are representative of the mean firing rate of each group. C, Proportion of cells with a firing frequency $>0.005\text{Hz}$ (black bars) vs $<0.005\text{Hz}$ (white bars); numbers are cell counts in each group. D, Individual values (CON open symbols, PNA black symbols) and mean \pm SEM and median (magenta line) for firing frequency across the duration of long-term recordings. Statistical parameters reported in Table 3.

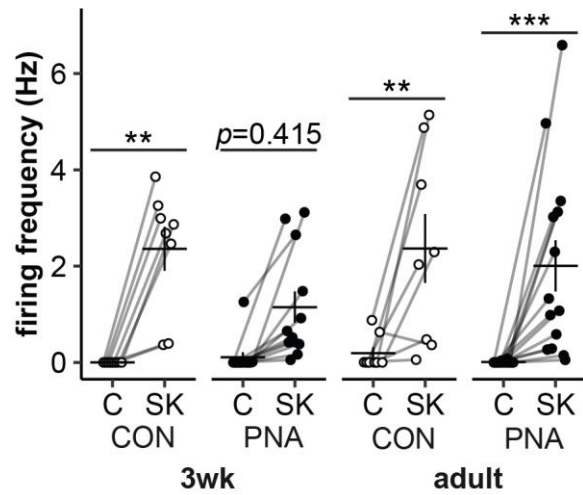


Figure 3. Senktide activates KNDy-neuron firing activity. Individual values and mean \pm SEM of firing rate during 5min control (C) and senktide (SK) periods. CON mice are shown in open symbols, PNA mice in black symbols. ** $p \leq 0.01$, *** $p \leq 0.001$. Statistical parameters in Table 4.

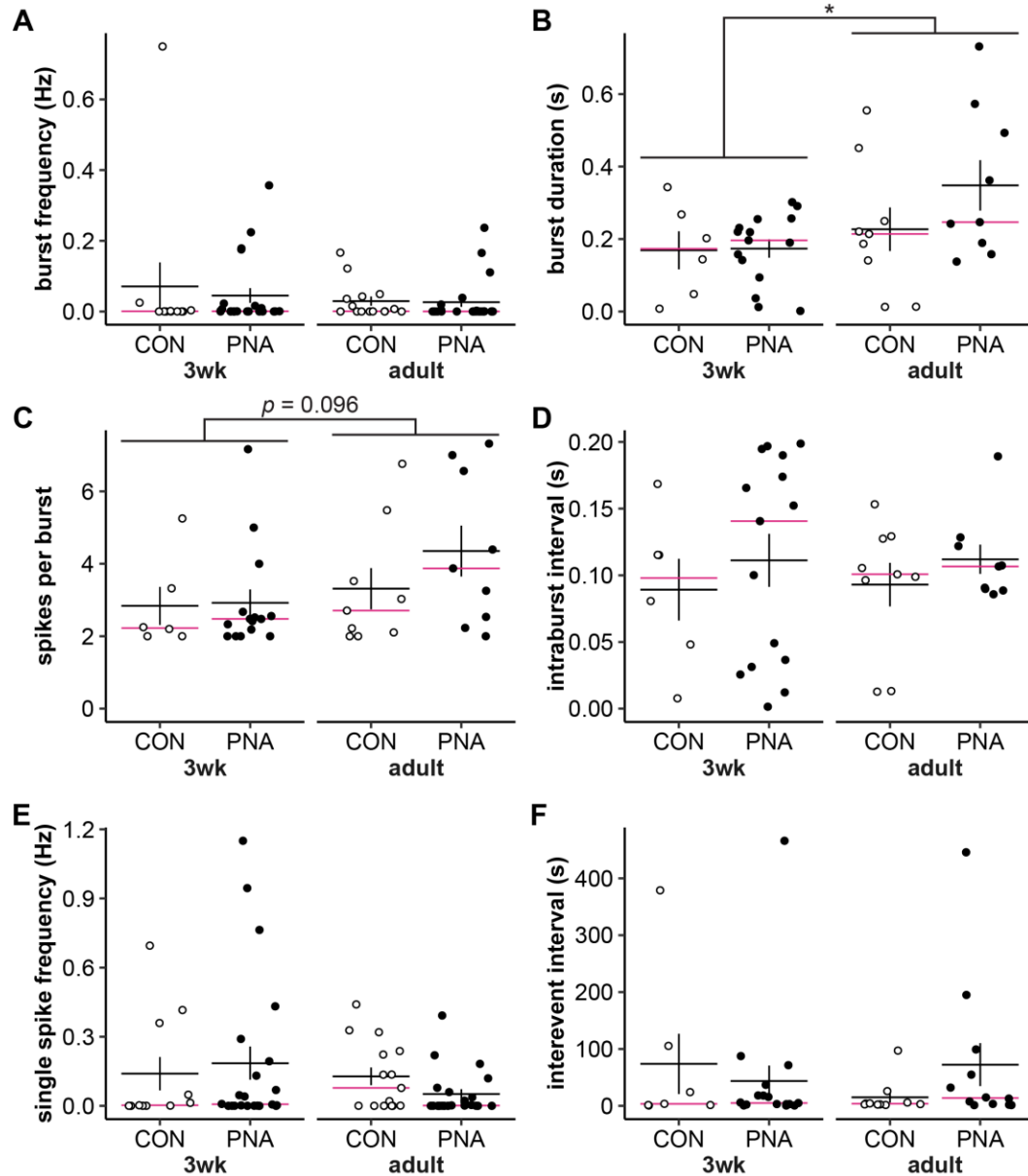


Figure 4. Effect of age and PNA treatment on burst parameters. A-F. Individual values (CON open symbols, PNA black symbols) and mean \pm SEM and median (magenta lines) burst frequency (A), burst duration (B), spikes per burst (C), intraburst interval (D), single spike frequency (E), and interevent interval (F). B, C, D. Burst parameters are only calculated for cells with at least one burst; 3wk-CON n=6 cells from 5 mice in 4 litters, 3wk-PNA n=15 cells from 10 mice in 5 litters, adult-CON n=9 cells from 8 mice in 5 litters, adult-PNA n=9 cells from 8 mice in 5 litters. F. Calculating interevent interval also requires multiple events, 3wk-CON n=7 cells from 6 mice in 5 litters, 3wk-PNA n=17 cells from 10 mice in 5 litters, adult-CON n=10 cells from 10 mice in 6 litters, adult-PNA n=12 cells from 9 mice in 5 litters; * $p < 0.05$. Statistical parameters in Table 5.

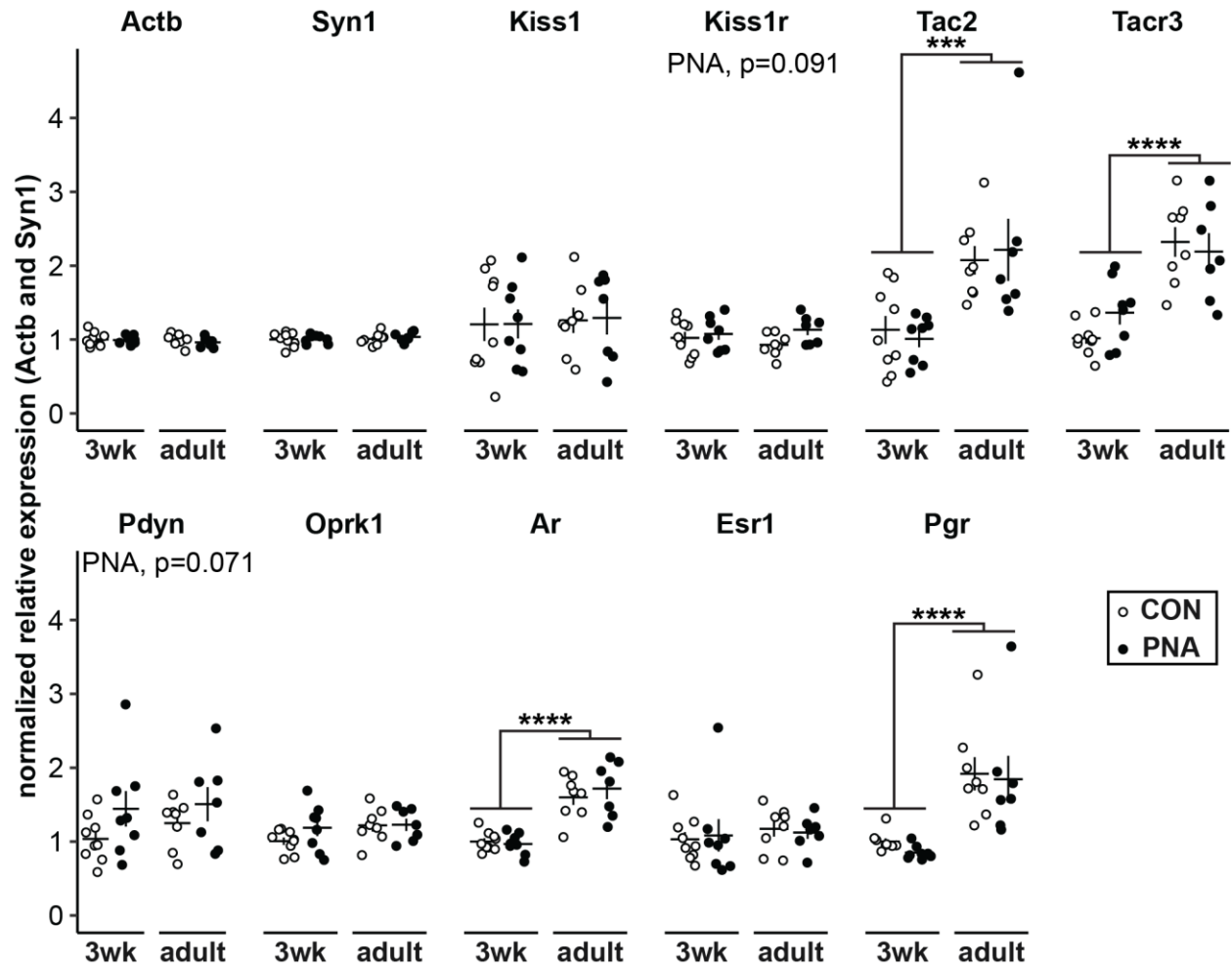


Figure 5. Effect of age and PNA treatment on arcuate nucleus mRNA transcripts. Individual values (CON open symbols, PNA black symbols) and mean \pm SEM for *Actb*, *Syn1*, *Kiss1*, *Kiss1r*, *Tac2*, *Tacr3*, *Pdyn*, *Oprk1*, *Ar*, *Esr1*, and *Pgr* mRNA isolated from arcuate nucleus tissue punches. Statistical parameters are reported in Table 6. ***p<0.001, ****p<0.0001

Extended Data 1. Code used to detect and analyze events in Igor Pro (coding-project) and for data analysis in R (PNA-KNDy).